



# Impact of weather regime on projected future changes in streamflow in a heavy snowfall area of Japan

Masamichi Ohba<sup>1</sup> · Ryosuke Arai<sup>1</sup> · Yasushi Toyoda<sup>1</sup> · Takahiro Sato<sup>1</sup>

Received: 27 May 2021 / Accepted: 21 January 2022 / Published online: 1 February 2022  
© The Author(s), under exclusive licence to Springer-Verlag GmbH Germany, part of Springer Nature 2022

## Abstract

Future changes in river discharge driven by climate change are expected to affect various water-resource sectors. In this study, we investigated the influence of climate change on streamflow in a heavy snowfall area of mountainous central Japan using hydrological model simulations driven by climate projections obtained from the d4PDF database. We projected an increase in snowmelt discharge during winter and a decrease in spring, along with a general decrease in water resources and an increase in the frequency of annual maximum daily discharge during winter because of increasing future snowmelt. Self-organizing maps (SOMs) were then applied using atmospheric data to study the linkage between streamflow and weather regime patterns (WPs) in future and present climate scenarios. The SOM analysis suggested that the impacts of climate change on streamflow varied by WP. The increase in future winter discharge was due to the strengthening of impacts of certain WPs, causing snowmelt. However, the decrease during spring could be due to changes in the predominant discharge-related WPs resulting from a decreasing snowpack. The obtained results can be useful information for considering adaptation strategies for sustainable management of water resources in heavy snowfall areas that must meet both economic and environmental demands.

**Keywords** Climate change · Hydrological model · Weather regime patterns · Self-organizing map · Snowmelt flood · Regional climate modeling

## 1 Introduction

Projected precipitation and river discharge are important sources of information for water resource utilization and the mitigation of floods and droughts (Vörösmarty et al. 2000; Milly et al. 2002; Nohara et al. 2006). In recent decades, many hydrological modeling studies have assessed the expected impacts of climate change on hydrological regimes and water availability (e.g., Arnell 1999; Sperna Weiland et al. 2012), given the potential consequences for freshwater ecosystems, water quality, and human water uses. For example, hydropower management requires daily to seasonal production planning, optimization, and long-term investment planning, all of which must account for changes in streamflow.

State-of-the-art regional climate model projections show that changes in average precipitation over Japan are likely

to be slight, while the frequency of extreme rainfall events is expected to increase (Kawase et al. 2019; Ohba and Sugimoto 2019). Although snowfall over Japan is expected to decrease overall, rainfall and extreme snowfall events are projected to increase in coastal areas of the Hokuriku region (on the Japan Sea side of central Japan), inland areas of Hokkaido (northern Japan), and mountainous areas of central Japan (Kawase et al. 2016; Sasai et al. 2019; Ohba and Sugimoto 2020). Such trends will affect hydropower generation through changes in mean annual river discharge, shifts in seasonal flow, and increases in streamflow variability. Therefore, the impact of climate change on specific hydropower plants depends on local changes in these hydrological characteristics, and projections of future hydropower generation are subject to uncertainties in projected precipitation and river discharge (Markoff and Cullen 2008). Increased winter streamflow, smaller and earlier spring floods, and reduced summer streamflow have already been observed in snow-dominated basins worldwide (Clow 2010; Korhonen and Kuusisto 2010; Tan et al. 2011).

Japan experiences some of the heaviest snowfalls in the world (Kazama et al. 2008). Changes in precipitation

✉ Masamichi Ohba  
oba-m@criepi.denken.or.jp

<sup>1</sup> Central Research Institute of Electric Power Industry (CRIEPI), 1646 Abiko, Abiko, Chiba 270-1194, Japan

intensity, snow cover, and snowmelt processes in mountainous regions like Japan have the potential to cause dramatic changes in river discharge, particularly as Japanese rivers tend to be short and high-gradient. However, few studies have predicted river discharge using hydrological models forced by high-resolution climate data, with a focus on snow-water resources and river discharge in heavy snowfall areas of Japan. Furthermore, because day-to-day weather-regime patterns (WPs) result in different precipitation scenarios or snowmelt processes, the resulting changes in streamflow due to climate change may also differ by weather condition. Hydro-climatological research focusing on the factors of atmospheric circulation can therefore improve the understanding of climate change impacts.

River discharge can be affected by synoptic-scale atmospheric circulation drivers with a nonlinear relationship to local atmospheric variables. The background weather conditions at the synoptic scale determine the precipitation type (rainfall or snowfall) events on timescales of one day to one week. Classification of synoptic WPs using the statistical properties of local meteorological variables provides insight into the origins of the discharge. Previous studies (Ohba and Sugimoto 2019, 2020) have used WP classification to identify the dominant extreme precipitation patterns (Ohba et al. 2015; Brigode et al. 2013) to discuss the change in impact of each pattern under climate change conditions. Climate change impacts on streamflow may vary by WP, leading to seasonal variations in future river discharge. In this study, we applied a WP classification technique to investigate the impacts of climate change on the linkage between streamflow and synoptic WPs from winter to spring for a river in a heavy snowfall area of Japan and to study future projections in discharge under climate change. Future changes in discharge were then evaluated with respect to related climatological/meteorological variables in a WP context.

## 2 Data and methods

### 2.1 Atmospheric data

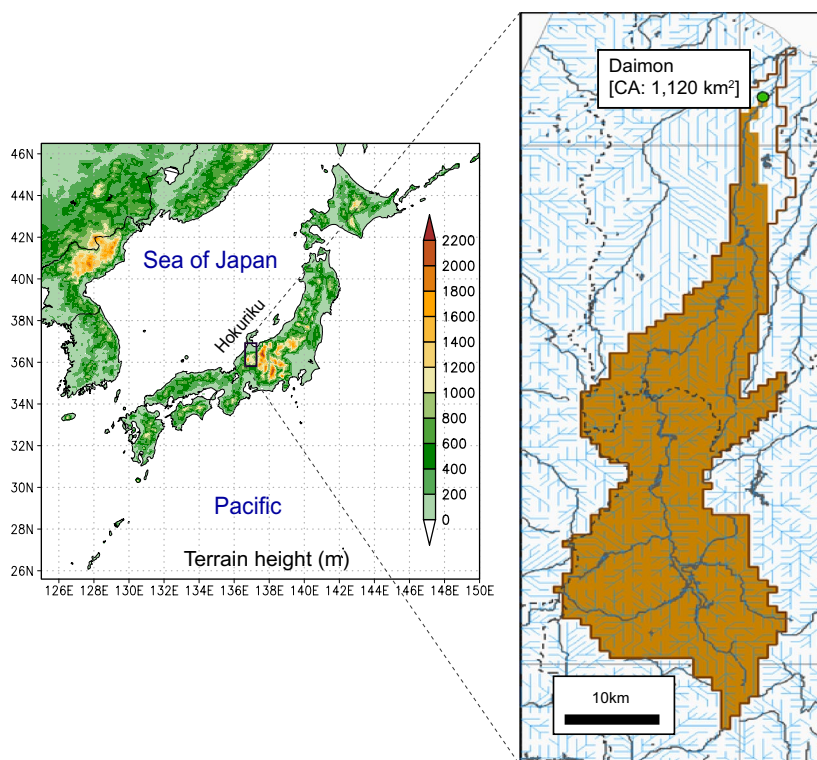
Simulated atmospheric data for historical and projected climatic conditions were taken from the d4PDF datasets (Mizuta et al. 2017). These consist of outputs obtained from a general circulation model (d4PDF-GCM) that was dynamically downscaled for the Japanese region using a regional climate model (d4PDF-RCM), with horizontal grid spacing of 60 and 20 km, respectively. Climate change impacts were analyzed using six-member historical simulations (1951–2010) and six six-member (six cases for each one-member ensemble, described below) +2 K (2031–2090) and +4 K (2051–2110) future-climate projections. The ensemble members were obtained from the perturbed

initial and lower boundary conditions of a 60-km GCM. The +2/+4 K simulations simulate a world in which the global mean temperature has increased by +2 K/+4 K since pre-industrial conditions. For the +2 K and +4 K future-climate simulations, climatological sea surface temperature (SST) warming patterns obtained from the six climate models (CCSM4, MIROC5, MPI-ESM-MR, HadGEM2-AO, GFDL-CM3, and MRI-CGCM3, contributing to Coupled Model Intercomparison Project Phase 5) were added to observational SSTs after removing long-term trends. The SST difference between RCP8.5 and historical simulations was used as the warming pattern. By adding perturbations to each pattern, a large number of ensemble simulations were conducted. The sea ice was adjusted to be consistent with the SST. The external forcing factors, such as greenhouse gas concentrations, were given as the values for 2090 (2040) in the RCP8.5 scenario for +4 K (+2 K) simulations. The degree of warming was set to remain constant throughout the simulation period. For the future climate projections (+2 K and +4 K respectively), a total of six members were used in this study—one member for each of the future climate simulations using the six-model warming SST pattern. The same ensemble members were used for the river discharge simulations and as input data to the SOM. Details of the experimental setup for these simulations are described in Kawase et al. (2016) and Mizuta et al. (2017). These data have already been used for boundary forcing of hydrological models for future flood projection (Tachikawa et al. 2017; Ishii and Mori 2020). The detailed validation of simulated precipitation in d4PDF was available for winter (Kawase et al. 2016; Ohba and Sugimoto 2020) and summer (Endo et al. 2017; Kawase et al. 2018; Ohba and Sugimoto 2019), respectively.

### 2.2 Target region

We evaluated the impact of climate change on snowmelt discharge at a watershed scale within the Shogawa River basin in mountainous central Japan, where snowmelt runoff is expected to be particularly extreme in d4PDF-RCM (Ohba and Kawase 2020). The Shogawa River is a Class A river (a river classification in Japan designated by the River Law that is applied to rivers deemed to be important to Japan's economy and the conservation of nature within Japan) with a 115 km long trunk channel and a basin area of 1189 km<sup>2</sup>, originating from Mount Eboshi in Takayama City, Gifu Prefecture (elevation 1625 m) and flowing northward into Toyama Prefecture, where it empties into the Japan Sea. Most of the basin is designated as a “special heavy snowfall area”, which in Japan refers to areas where the average cumulative daily snow depth is > 5000 cm. We focused on the Daimon River basin (1120 km<sup>2</sup>), which covers most of the Shogawa River basin (Fig. 1).

**Fig. 1** Topographic map of Japan and location of the Daimon River basin study area



### 2.3 Hydrological model

We used the HYDrological Evaluation with Evapotranspiration Modeling System (HYDREEMS) as a hydrological model to simulate river discharge (Toyoda 2006; Asaoka et al. 2010; Arai et al. 2020; Ohba et al. 2020). This is a distributed hydrological runoff model that analyzes river flow using the kinematic wave method and soil and groundwater flow based on tank models. The target watershed was divided into a 1 km square mesh. In this model, tanks corresponding to each hydrological process are arranged vertically in each mesh and connected to each other in order to accurately represent the processes of rainfall to the surface, infiltration through the soil, and discharge into rivers (Fig. S1). Therefore, the rainfall given to HYDREEMS flows down to the connected vertical and horizontal tanks. Each hydrological process is modeled as follows: rainfall interception, a function of forests, is modeled as a "vegetation tank"; snowfall and snowmelt processes are modeled as a "snow tank"; soil infiltration processes are modeled as "surface tank," "unsaturated tank," and "underground tank"; and runoff processes in river channels are modeled as a "river channel tank." In addition to the water balance, the model also analyzes heat and radiation balances, and thus faithfully represents evapotranspiration, snow accumulation, and snowmelt processes (see Toyoda et al. 2015; Arai et al. 2020 for further details). Snowmelt processes were evaluated by considering five components: radiation balance, sensible heat, latent heat,

rainwater transfer heat, and ground heat. The validation of the simulated discharge by the model in the target region is discussed in the supplementary material (Fig. S2).

Six long-term simulations of streamflow were conducted under each of the climates. Six simulations were extracted for each of the present and future climate ensembles. For this extraction, we calculated the 50-year return value of precipitation and then selected the ensemble member whose value was closest to the median among the ensembles. For the future climate simulations, one simulation was extracted from each of the six ensemble sets based on different SST warming patterns. Atmospheric variables (precipitation, sea level pressure, pressure, specific humidity, relative humidity, downward short- and long-wave radiation, wind speed, and surface temperature) from d4PDF were used as boundary input variables for the hydrological model. However, a compensation was introduced for atmospheric temperature and other meteorological data in d4PDF (Arai et al. 2020; Ohba et al. 2020) according to elevation data at the HYDREEMS spatial resolution (1 km) to account for the elevation dependence of snow accumulation and melting processes.

### 2.4 SOM technique

Self-organizing map (SOM; Kohonen 1982) is a kind of artificial neural network built on unsupervised learning that can effectively classify various nonlinear patterns. This can project high-dimensional data onto a visually comprehensible

two-dimensional map and has been used in previous climatological studies to obtain spatially organized WPs (see Ohba et al. 2016a for further details). Previous studies have examined the connections between synoptic-scale WPs and local meteorological variables (Cavazos 1999; Cassano et al. 2007; Polo et al. 2011; Singh et al. 2014; Ohba et al. 2015), and these linkages have been successfully employed for weather forecasting (Cavazos et al. 2002; Chattopadhyay et al. 2008; Ohba et al. 2016b, 2018) and climate characterization (Reusch et al. 2007; Ohba 2019; Johnson and Feldstein 2010). These studies have successfully used SOMs to extract clearly defined WPs from nonlinear atmospheric elements. The potential benefits of using this technique for climatology have been mentioned in previous studies (Reusch et al. 2007; Gibson et al. 2017). The classification of WPs by SOM could be effective in specifying the complex nonlinear interrelationships between climate factors and synoptic WPs. In this study, we used a batch version of the SOM algorithm and a Gaussian-type neighborhood function with a torus-type SOM (Ito et al. 2000) instead of a conventional SOM because the former has no map edges. For further details of the SOM projection process, see Gibson et al. (2017) and Doan et al. (2021).

In order to classify synoptic WPs with minimum computational costs, daily-averaged surface zonal and meridional winds obtained from d4PDF-GCM were used as the input vectors for SOM. Raw surface-wind vectors within a specific region (123°–148° E, 26°–48° N) were interpolated into a grid of 1 degree in both latitude and longitude and used for SOM. By using just the horizontal surface wind vector, the SOM effectively analyzed near-surface atmospheric circulation patterns. For simplicity, only +4 K and the present climate simulations were used in SOM analysis. Each element of the array was represented as a node with a single reference vector, with each reference vector representing a generalized pattern of input vectors. Each reference vector had 1100 (25° of longitude  $\times$  22° of latitude  $\times$  2 variables) elements, and the number of input vectors was 131,040 (182 days  $\times$  60 years  $\times$  12 ensembles for the historical and future simulations; six-member historical and six-member future climate simulations were used to make the SOM). SOM training extracts generalized patterns from the input data into a reference vector. In this study, a 15  $\times$  15 grid SOM was used to classify the input data into 225 WPs. By mapping the input data to the best matching pattern, we grouped the data by pattern, which allowed us to perform statistical and composite analysis. Other atmospheric variables, such as sea level pressure (SLP), and other SOMs with different numbers of nodes, such as 20  $\times$  20, were also tested to ensure that they did not significantly affect the results. The present and +4 K climate simulations were used simultaneously to train one SOM to directly compare the impact of climate change on river discharge under the same WP.

## 3 Results

### 3.1 Future discharge changes in a special heavy snowfall area

Figure 2 shows hydrographs of annual river discharge in the study area for the present and two future climates derived from the long-term ensemble of the hydrological model simulations driven by d4PDF-RCM data. Climate change clearly resulted in significant changes in the seasonal evolution of mean discharge. The peak discharge associated with spring snowmelt decreased and shifted earlier, with a maximum mean peak flow rate of  $\sim 250$  m<sup>3</sup>/s (early May) in the present climate changing to  $\sim 200$  m<sup>3</sup>/s (mid-April) in the +2 K climate and  $\sim 150$  m<sup>3</sup>/s (early April) in the +4 K climate. This shift toward an earlier discharge peak was similar to previous results obtained in other regions (Mote et al. 2003; Surfleet and Tullos 2013), although the intensity of the change was different. While there was some variation between ensembles, the overall trends were consistent.

The seasonal evolution of basin-averaged snow water equivalent (SWE), snowfall, and precipitation values are shown in Fig. 3. The shift of the discharge peaks seen in Fig. 2 were likely due to decreases in winter SWE of  $\sim 35\%$  at +2 K and  $\sim 70\%$  at +4 K (Fig. 3a) because of the phase shift from snowfall to rainfall under rising temperature conditions. Winter snowfall and total precipitation in the region also tended to decrease with rising temperature (Fig. 3b and c), although this effect was small relative to the change in SWE (i.e., the blue/green/red slopes in Fig. 3a are steepest compared with Fig. 3b and c). The decrease in precipitation thought to be due to the weakening of the winter monsoon (Fig. S5; Hori and Ueda 2006). These results are consistent with changes in river discharge (Fig. 2). The corresponding annual flow duration curves (Fig. 4) show that water resources decreased with climate change for up to 100 days, though there was little difference between the present and warming climates beyond this point.

The monthly frequency of annual maximum daily flow (Fig. 5) tended to be particularly high from April to May during the present climate, when snowmelt runoff was abundant. On the other hand, in future climates, this was greatly reduced in spring and greatly increased in winter, when flooding is rarely experienced in the present climate. Such changes could affect both seasonal variations in average flow and seasonal flood occurrence, especially from winter to spring.

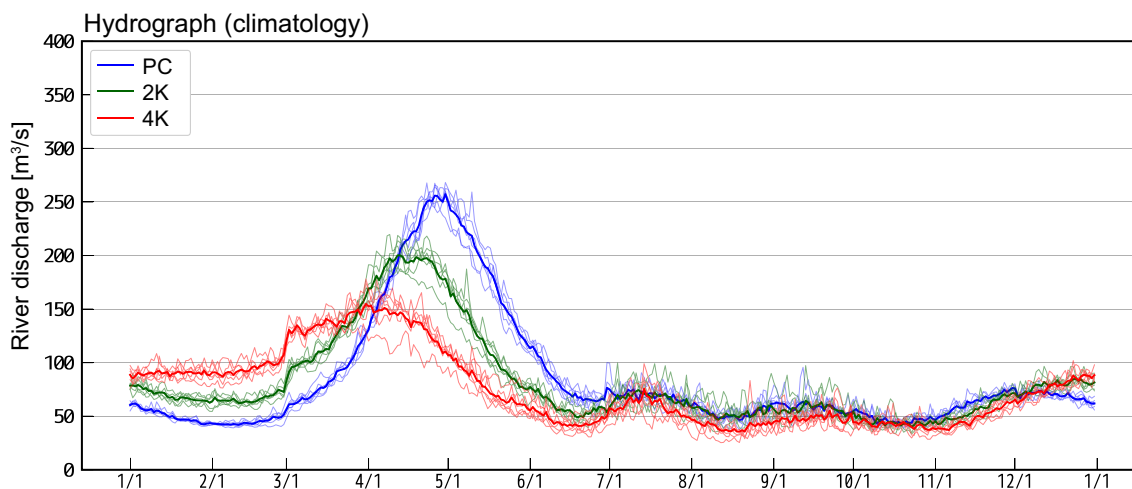


**Fig. 2** Annual hydrographs obtained from simulated discharge for present (blue), +2 K (green), and +4 K (red) climate simulations. Thin and thick lines represent ensembles and ensemble means, respectively

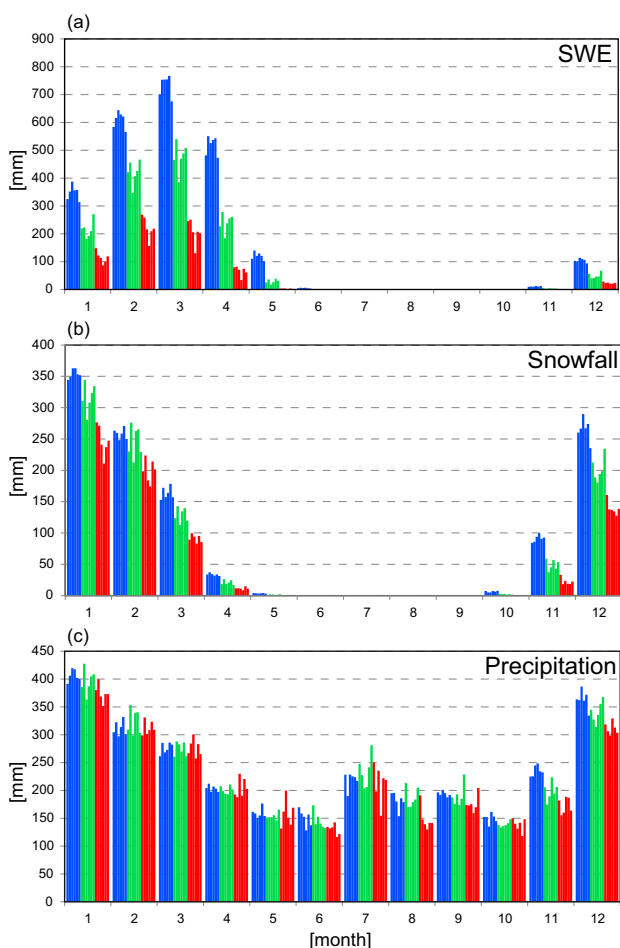


**Fig. 3** Seasonal means of regionally averaged daily **a** SWE, **b** snowfall, and **c** precipitation for six ensembles of present (blue), +2 K (green), and +4 K (red) climate simulations

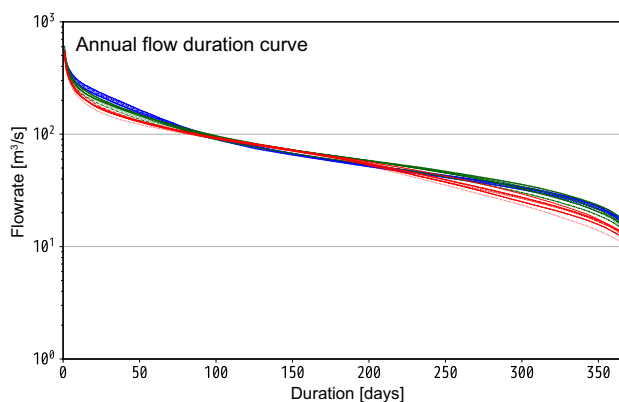


**Fig. 4** Annual flow duration curve obtained for six ensemble simulations of present (blue), +2 K (green), and +4 K (red) climate simulations. Thin and thick lines represent ensembles and ensemble means, respectively

### 3.2 Weather regime patterns leading to changes in discharge

As various WPs occur within seasons, specifying whether a given WP will produce a river discharge in current/future climate simulations is difficult; thus, classification of WPs helps us to better understand the link between WPs and river discharge. We therefore focused on further analyzing data from December 1 to May 31 (winter to spring in Japan, when future changes were most pronounced).

Large-scale climatological features of atmospheric circulation and their future changes during winter and spring in Japan are shown in Figs. S5 and S6, respectively. Synoptic weather systems bringing winter precipitation differ among the inland areas of mainland Japan, along the Pacific Ocean and the Sea of Japan (Ando and Ueno 2015;

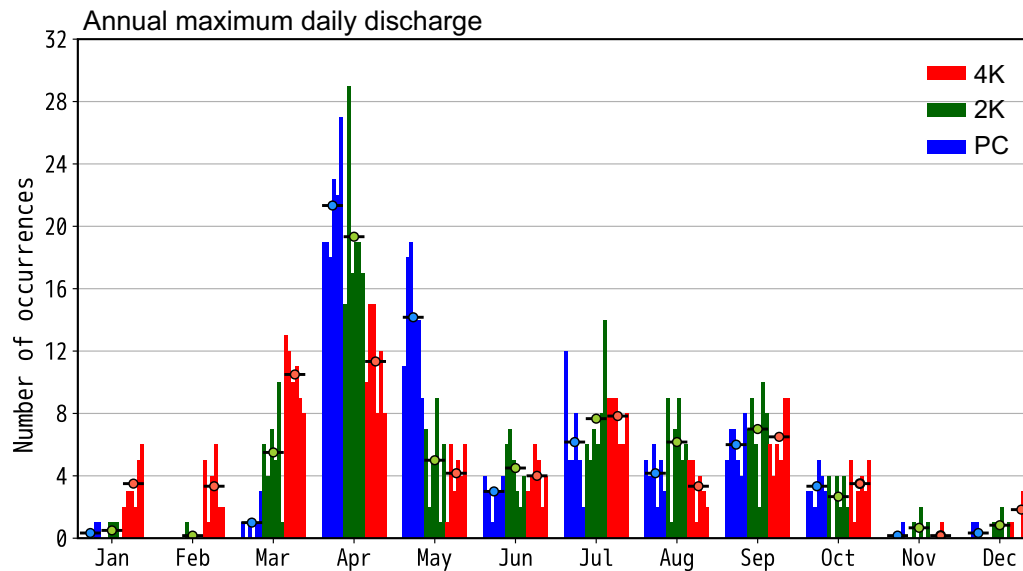


**Fig. 5** Frequency of simulated annual maximum daily discharge for present (blue), +2 K (green), and +4 K (red) climate simulations. Horizontal lines represent ensemble averages

Kawase et al. 2018). According to statistical analyses, the cause of the heavy snowfall is strong northerly–northwesterly winds blowing from Eurasia along the Sea of Japan that are regarded as an intensified climatological winter monsoon (Tachibana 1995). Weaker winds and a less pronounced pressure gradient occur in spring relative to winter. In spring, the weather changes in cycles of a few days as high- and low-pressure systems pass near Japan alternately from west to east. On the east (west) side of the low-pressure system, the temperature rises (falls) as warm (cold) air from the south (north) flows into Japan. In the latter half of spring, the number of high-pressure days gradually increases, as does the sunshine duration.

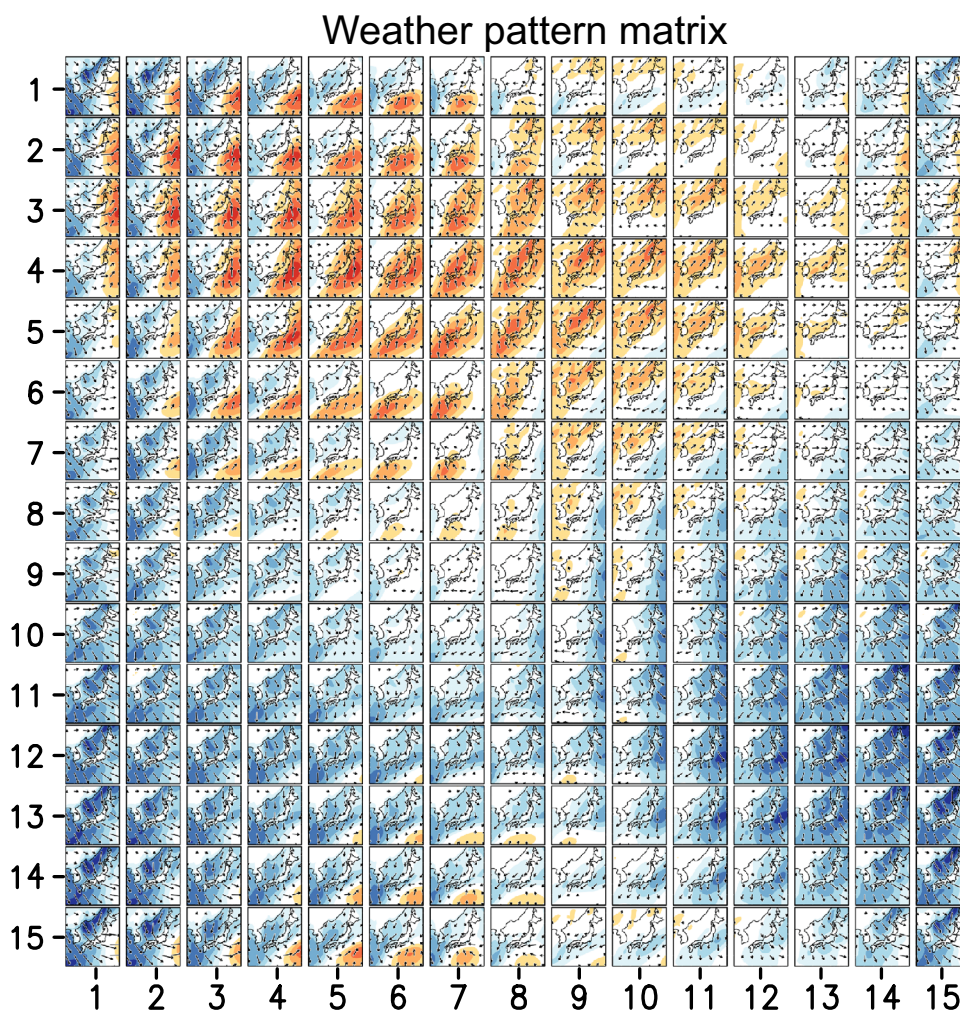
Figure 6 shows the matrix of WP derived from the SOM analysis. The day-by-day weather conditions from December to May around Japan were classified into 225 WPs represented on a  $15 \times 15$  SOM where meridional winds are indicated by red-blue shadings. The classified WPs featuring southerly (northerly) winds are located near (far from) the upper center of the map. WPs corresponding with cyclonic circulation are located in the top left. The bottom-right to bottom-left sides are covered by WPs in relation to cold air outbreaks from the Eurasian continent. Since the surface wind vector was selected as the input variable for the SOM, it was easy to visually observe the strong influence of monsoonal winds on precipitation during the season.

The peak flow rate in this basin relative to the WP was delayed by approximately one day. The linkages between river discharge and WPs were identified using the SOMs for December–February (DJF) and March–May (MAM). Figures 7 and 8 show the daily mean (+1 d) river discharge in

each SOM for the present/+4 K climate simulations in DJF and MAM, respectively. The river discharge plotted here is the node mean discharge occurring at a particular node (WP). It is calculated by averaging the discharge for all days within the time period of interest that are identified with the node of interest. By calculating this value for both climates, the difference in node mean discharge between climates can be calculated. Since the node mean discharge is calculated for all daily data whose WP is most similar to that of the target node, the discharge difference reflects the discharge change that occurs for a given circulation regime. Therefore, these differences in discharge are attributed to changes not related to circulation or frequency. These changes are due to changes in the thermodynamics and physics of the discharge associated with climate change, of which changes in precipitation and snowmelt should be major factors. This is a useful way to assess the thermodynamic changes in discharge associated with climate change.

In both seasons, it was evident that river discharge was strongly dependent on the WPs. During winter, a strong impact of WPs on river discharge was most apparent in the top-left region of the SOM in both present and future climates (Fig. 7a and b), with the future signal being stronger, and the annual maximum discharge sometimes occurring in the WPs. On the other hand, spring showed a roughly opposite trend (Fig. 8a and b), in which discharge and annual maximum discharge were significantly reduced in the WPs under climate change. Figures 7c and 8c show the differences in river discharge intensity between the future- and present-climate simulations. Overall, the response of the WP-discharge relationship to climate change clearly varied

**Fig. 6** WPs derived from the  $15 \times 15$  SOM nonlinear classification, based on horizontal surface wind vectors in d4PDF-GCM from winter to spring (December–May). Red and blue contours indicate northward and southward meridional winds, respectively



by season, with the difference between the future and present climate showing that the contrast between nodes was much more enhanced (reduced) in the future climate in winter (spring).

Unlike DJF (Fig. 7c), changes in river discharge in MAM (Fig. 8c) were more complex, with discharge increasing in the bottom left and decreasing in the upper center parts of the SOM. These results clearly showed the impact of synoptic weather conditions on discharge and future changes, demonstrating that WPs have different impacts on discharge and future changes also vary by WP. Five WPs (WP1–5) marked in Figs. 7c and 8c show relatively large changes in river discharge intensity in response to climate change; these are further highlighted in Figs. 9 and 10.

Figure 9 shows the surface temperature anomaly (difference from climatological mean) and rainfall in the present climate simulation and the future difference in rainfall for WP1 and WP2 in DJF. In these WPs, warm humid air from the subtropics flows into Japan, causing higher temperatures and rainfall; these may be the dominant snowmelt WPs during this season. WP1 is responsible for an

extratropical cyclonic circulation over central Japan, which brings strong air intrusion into the target area from the south. This WP frequently results in heavy rainfall over the region when a low-pressure system and corresponding fronts pass through (Ando and Ueno 2015). When a cyclonic low with cold/warm front moves to the east, moist warm air sometimes flows toward the lows through warm fronts. This phenomenon has a pronounced effect on snowmelt in central Japan. In contrast, in WP2, the zonal pressure gradient was reversed from the climatological mean (Fig. S5), and southerly winds flowed into central Japan. WP1 showed more precipitation than WP2. The right panel of Fig. 9 shows the corresponding daily mean snowmelt and rainfall in the basin for WPs 1 and 2. Winter rainfall on snowpack ("rain-on-snow") can enhance transfers of latent and sensible heat that hasten snowmelt (Marks et al 1998; Corripio and López-Moreno 2017). For these WPs in this season, snowmelt associated with sensible heat and latent heat are comparable, and snowmelt due to rain-on-snow is the main cause of streamflow.

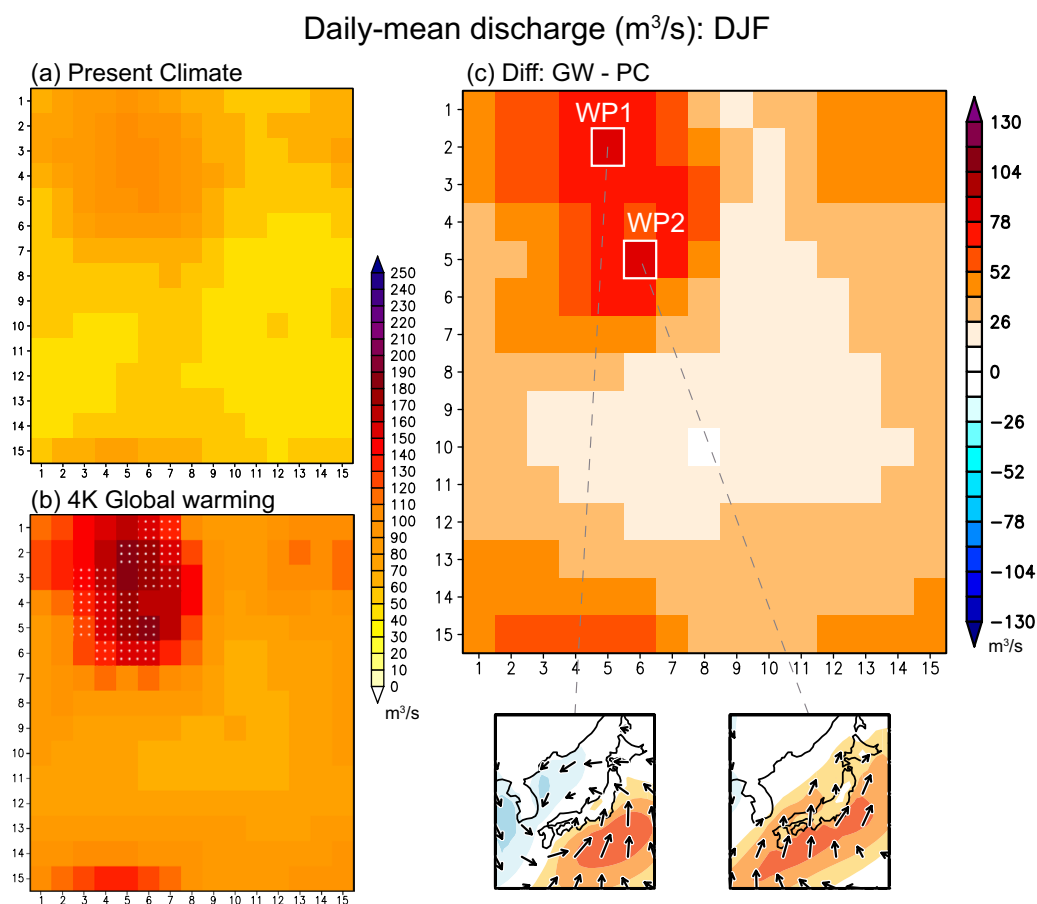


**Fig. 7** Simulated river discharge at each SOM node during winter (December–February) for **a** present climate, **b** +4 K future climate, and **c** difference between the two. Boxes denote nodes with the high-

est increase in river discharge for weather regime patterns WP1 and WP2. White dots indicate the number of occurrences (ensemble mean) of annual maximum daily discharge exceeding 2

Under climate change, the rainfall over Japan associated with WP1 has increased significantly. The right panel of Fig. 9 shows that both increased rainfall and snowmelt were responsible for streamflow enhancement in WP1, while only snowmelt was responsible in WP2. This may be due to the phase change from snowfall to rainfall, associated with rising temperature, being less pronounced in WP2 because of the stronger warm air advection in the present climate (already exceeding the freezing point).

Figures 10 show results for WP3–5 in MAM. WP3 is a quiet-warm-sunny pattern, in which snowmelt is mainly caused by sensible heat. WP4 is a moist, warm air inflow pattern with simultaneous rainfall, relatively similar to WP2 in winter but with more pronounced snowmelt in spring. Rain-on-snow results in snowmelt due to sensible and latent heat in WP4, producing higher snowmelt discharge than in WP3. WP5 corresponds to extratropical cyclonic circulation over the Pacific coast of northeast Japan, which provides cold air intrusion from the north into the southwestern regions of Japan. In the current climate, this WP results in local snowfall (Iwamoto et al. 2008; Yamazaki et al. 2019)

along with intensified cold air outbreaks but not rainfall because the air temperature tends to be below freezing.

Under climate change, in both WP3 and WP4, SWE was reduced due to the temperature increase caused by climate change, and snowmelt discharge was significantly reduced. As for WP5 (Fig. 10c), increased temperature leads to a shift from snowfall to rainfall, which shows weak discharge in the present climate but is enhanced in the future climate because of the increased rainfall, mitigating the discharge reduction in spring. These results indicate that the reduction in future climate snow amounts may result in changes in the dominant discharge-related WPs (Fig. 8a and b). The integration of these changes seen in WPs is largely in line with the projected future changes of discharge (Fig. 3).

## 4 Conclusions

This is the first study to apply hydro-climatological/meteorological analysis to projected changes in river discharge and related WP characteristics under climate change projections



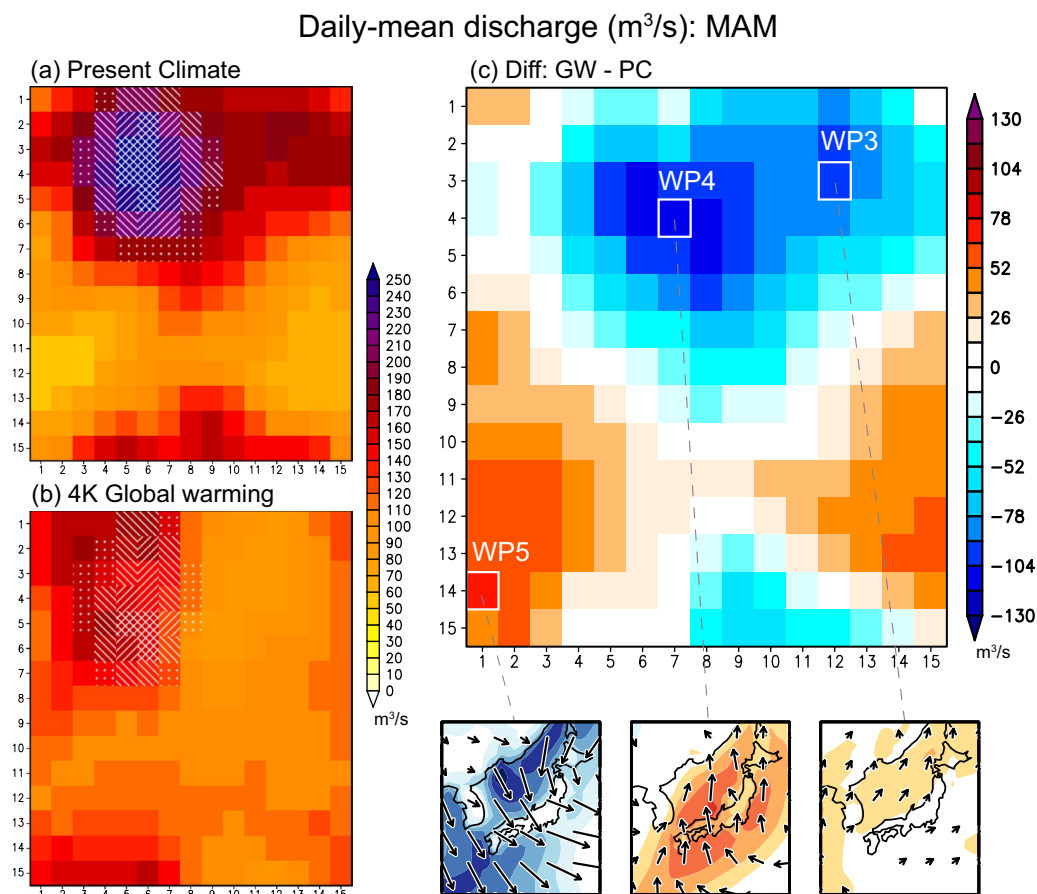


**Fig. 8** Simulated river discharge at each SOM node during spring (March–May) for **a** present climate, **b** +4 K future climate, and **c** difference between the two. Boxes denote nodes with the highest increase in river discharge for weather regime patterns WP3, WP4,

and WP5. White dots, left-inclined, right-inclined, and cross-hatched lines indicate the number of occurrences (ensemble mean) of annual maximum daily discharge exceeding 2, 5, 10, and 20, respectively

in a special heavy snowfall area of Japan. Our results suggest (1) a general decrease in future discharge in the study area, especially during spring, due to decreasing SWE in winter, related to increased air temperature, (2) a general decrease in water resources, and (3) an increase in the frequency of annual maximum daily discharge during winter because of increased future snowmelt.

In order to understand the differences in the climate change impacts among synoptic WPs, we also investigated the complex relationship between possible future changes in discharge and synoptic WPs. The impact of synoptic WPs on discharge from winter to spring was dramatically altered in future climate situations. The differences in the response to various WPs are likely due to changes in the freezing point line, resulting in increased rainfall (decreased snowfall) and snowmelt. Changes in the seasonal cycle of discharge were caused by the integration of these nonlinear changes into the WP effects. The results also demonstrate the benefits of WP comparisons in terms of climate change for improving our understanding of future changes in streamflow. Our

methods were effective for analyzing the impacts of WPs on streamflow and their changes under climate change conditions, enabling enhanced interpretability of climate change impact assessments.

The results of the six simulations based on different SST warming patterns are in overall agreement, although the range of uncertainty is large. In addition, we studied future changes in river discharge by using hydrological simulations forced by regional climate simulations with a 20 km grid spacing, which roughly resolved Japan's complex mountains. Using a higher-resolution model ( $\sim 5$  km/2 km) will better reproduce rainfall and snowfall (Kawase et al. 2018), and thus further improve the projection of discharge. Future study should employ hydrological simulations with different cloud-resolving RCMs downscaled from different GCMs to more accurately evaluate uncertainties in discharge within Japan's complex mountainous terrain.

The projected changes to discharge characteristics, especially from winter to spring, are useful for evaluating detailed local climate impacts on environmental, social,

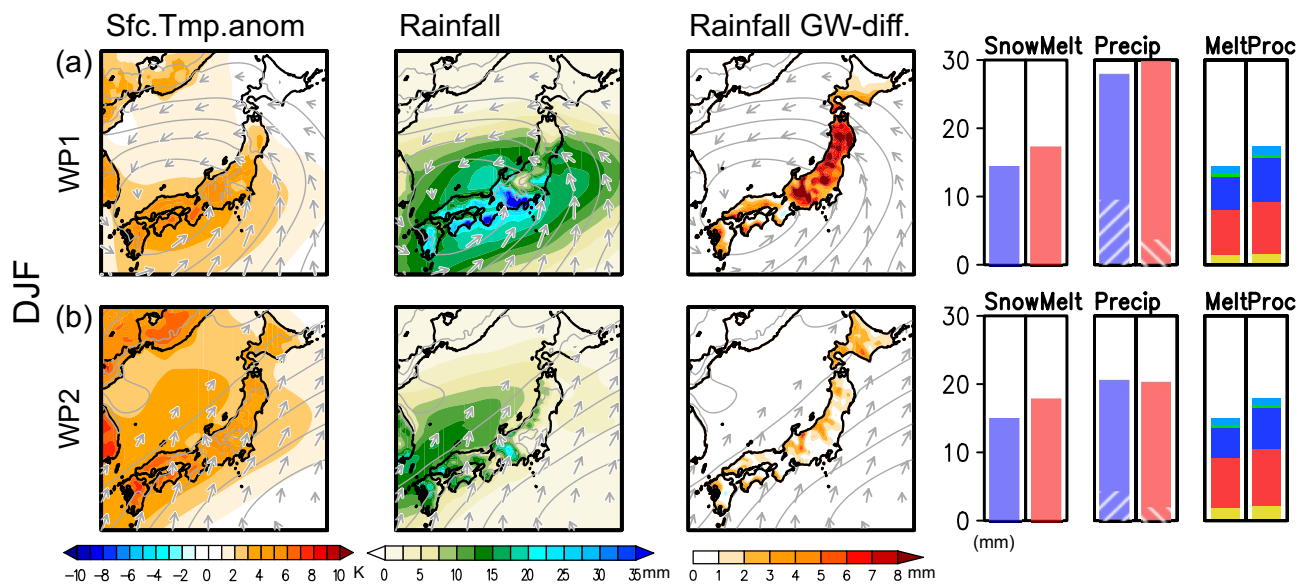


**Fig. 9** Winter surface temperature anomaly from the climatological mean, rainfall, and rainfall difference between future and present climate simulations for **a** WP1 and **b** WP2. Horizontal surface wind vectors (gray contours, 2 hPa interval) are based on SOM analysis and sea-level pressure from the present climate simulation. On the right, daily snowmelt (light blue, mm/day) and precipitation (light

red, mm/day) along with five snowmelt processes (yellow, radiation; red, sensible heat; dark blue, latent heat; green, ground heat; medium blue, rainfall heat) in the river basin in the present (blue) and +4 K future (red) climate simulations. Angled white lines within precipitation indicate snowfall

water resource management, and ecosystem sectors in this special heavy snowfall area. For example, hydropower potential could be affected by changes in river flow associated with variability of weather events causing snowmelt and precipitation (Troccoli et al. 2014). The management of water resources from winter to spring in mid-latitude heavy snowfall areas may have to be significantly altered in future. Continued efforts to accurately estimate water discharge for each river basin by using hydrological models is continuously necessary to better assess the climate change impacts and develop adaptation measures for future dam operations.

**Supplementary Information** The online version contains supplementary material available at <https://doi.org/10.1007/s00382-022-06163-x>.

**Acknowledgements** This study used d4PDF produced with the Earth Simulator jointed by science programs (SOUSEI, TOUGOU, SI-CAT, DIAS) of the Ministry of Education, Culture, Sports, Science and Technology (MEXT), Japan.

**Data availability** d4PDF is fully described and available at [http://www.miroc-gcm.jp/~pub/d4PDF/index\\_en.html](http://www.miroc-gcm.jp/~pub/d4PDF/index_en.html).

## Declarations

**Conflict of interest** The authors declare that they have no conflict of interest.

## References

- Ando N, Ueno K (2015) Occurrence tendency of heavy rainfall or snowfall in the inland district of Japan in winter. *Seppyo* 77:397–410 (**in Japanese with English abstract**)
- Arai R, Toyoda Y, Ohba M et al (2020) Climate change effects on snowmelt runoff in Shogawa River Basin. *J Jpn Soc Civ Eng G* 76:109–120
- Arnell NW (1999) A simple water balance model for the simulation of stream flow over a large geographic domain. *J Hydrol* 217:314–335. [https://doi.org/10.1016/S0022-1694\(99\)00023-2](https://doi.org/10.1016/S0022-1694(99)00023-2)
- Asaoka Y, Toyoda Y, Takeuchi Y (2010) The effect of the precipitation form discrimination method on river discharge estimation during winter. *Ann J Hydraul Eng* 54:421–426
- Brigode P, Mićović Z, Bernardara P et al (2013) Linking ENSO and heavy rainfall events over coastal British Columbia through a weather pattern classification. *Hydrol Earth Syst Sci* 17:1455–1473. <https://doi.org/10.5194/hess-17-1455-2013>
- Cassano JJ, Uotila P, Lynch AH, Cassano EN (2007) Predicted changes in synoptic forcing of net precipitation in large Arctic river basins during the 21st century. *J Geophys Res Biogeosci* 112:G4S49. <https://doi.org/10.1029/2006JG000332>
- Cavazos T (1999) Large-scale circulation anomalies conducive to extreme precipitation events and deviation of daily rainfall in northeastern Mexico and southeastern Texas. *J Clim* 12:1506–1523. [https://doi.org/10.1175/1520-0442\(1999\)012%3c1506:LSCACT%3e2.0.CO;2](https://doi.org/10.1175/1520-0442(1999)012%3c1506:LSCACT%3e2.0.CO;2)
- Cavazos T, Comrie AC, Liverman DM (2002) Intraseasonal variability associated with wet monsoons in southeast Arizona. *J Clim* 15:2477–2490. [https://doi.org/10.1175/1520-0442\(2002\)015%3c2477:IVAWWM%3e2.0.CO;2](https://doi.org/10.1175/1520-0442(2002)015%3c2477:IVAWWM%3e2.0.CO;2)
- Chattopadhyay R, Sahai AK, Goswami BN (2008) Objective identification of nonlinear convectively coupled phases of monsoon

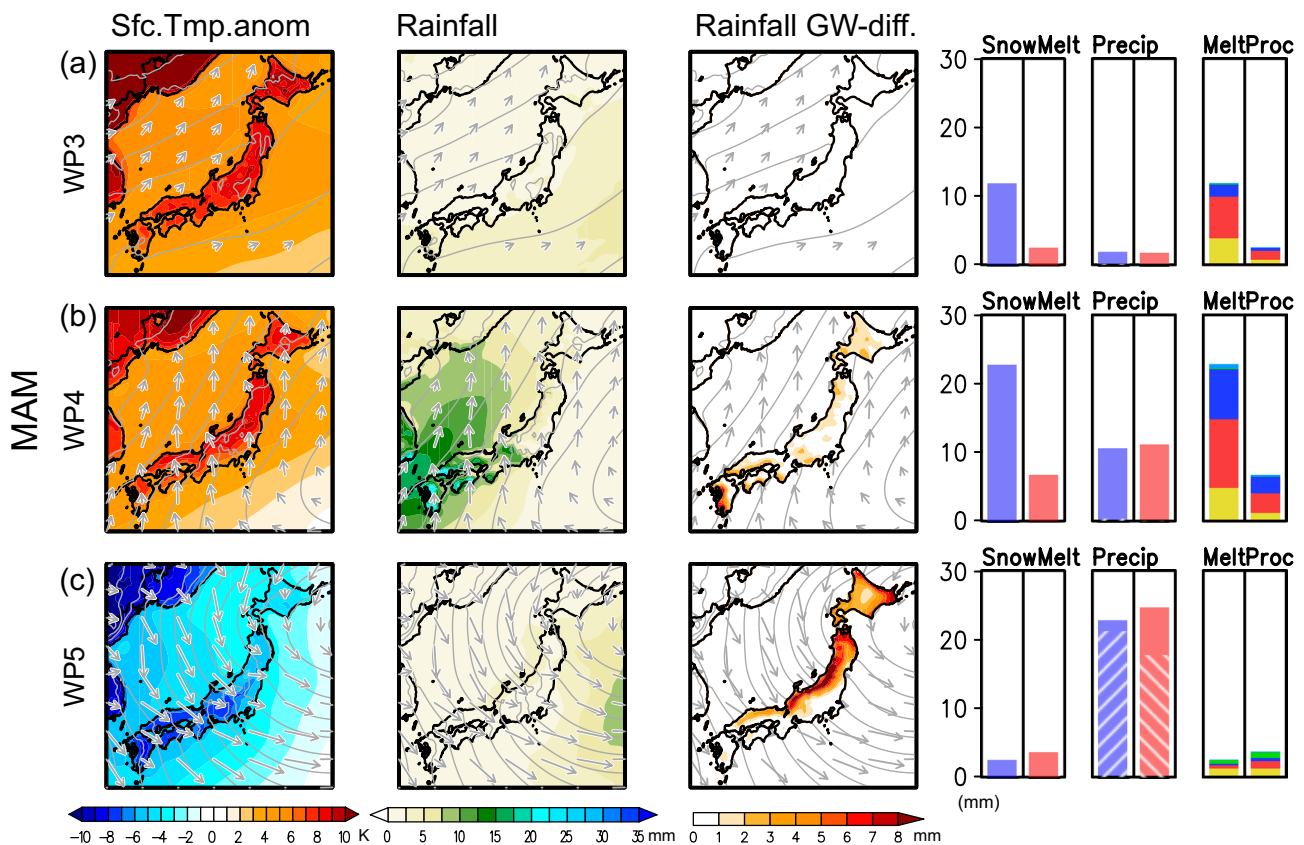


**Fig. 10** Spring surface temperature anomaly from the climatological mean, rainfall, and rainfall difference between future and present climate simulations for **a** WP3, **b** WP4, and **c** WP5. Horizontal surface wind vectors (gray contours, 2 hPa interval) are based on SOM analysis and sea-level pressure from the present climate simulation. On the right, daily snowmelt (light blue, mm/day) and precipitation (light

red, mm/day) along with five snowmelt processes (yellow, radiation; red, sensible heat; dark blue, latent heat; green, ground heat; medium blue, rainfall heat) in the river basin in the present (blue) and +4 K future (red) climate simulations. Angled white lines within precipitation indicate snowfall

intraseasonal oscillation: implications for prediction. *J Atmos Sci* 65:1549–1569. <https://doi.org/10.1175/2007JAS2474.1>

Clow DW (2010) Changes in the timing of snowmelt and streamflow in Colorado: a response to recent warming. *J Clim* 23:2293–2306. <https://doi.org/10.1175/2009JCLI2951.1>

Corripio J, López-Moreno JI (2017) Analysis and predictability of the hydrological response of mountain catchments to heavy rain on snow events: a case study in the Spanish Pyrenees. *Hydrology* 4:20. <https://doi.org/10.3390/hydrology4020020>

Doan VQ, Kusaka H, Sato T, Chen F (2021) S-SOM v1.0: a structural self-organizing map algorithm for weather typing. *Geosci Model Dev* 14:2097–2111. <https://doi.org/10.5194/gmd-14-2097-2021>

Endo H, Kitoh A, Mizuta R, Ishii M (2017) Future changes in precipitation extremes in East Asia and their uncertainty based on large ensemble simulations with a high-resolution AGCM. *Sola* 13:7–12. <https://doi.org/10.2151/sola.2017-002>

Gibson PB, Perkins-Kirkpatrick SE, Uotila P et al (2017) On the use of self-organizing maps for studying climate extremes. *J Geophys Res Atmos* 122:3891–3903. <https://doi.org/10.1002/2016JD026256>

Hori ME, Ueda H (2006) Impact of global warming on the East Asian winter monsoon as revealed by nine coupled atmosphere-ocean GCMs. *Geophys Res Lett* 33:L03713. <https://doi.org/10.1029/2005gl024961>

Ishii M, Mori N (2020) d4PDF: Large-ensemble and high-resolution climate simulations for global warming risk assessment. *Prog Earth Planet Sci* 7:58. <https://doi.org/10.1186/s40645-020-00367-7>

Ito M, Miyoshi T, Masuyama H (2000) The characteristics of the torus self-organizing map Proceedings 16th fuzzy system symposium Akita Japan Society for Fuzzy and Systems, pp 373–374

Iwamoto K, Nakai S, Sato A (2008) Statistical analyses of snowfall distribution in the Niigata area and its relationship to the wind distribution. *Sola* 4:45–48. <https://doi.org/10.2151/sola.2008-012>

Johnson NC, Feldstein SB (2010) The continuum of North Pacific sea level pressure patterns: Intraseasonal, interannual, and interdecadal variability. *J Clim* 23:851–867. <https://doi.org/10.1175/2009JCLI3099.1>

Kawase H, Murata A, Mizuta R et al (2016) Enhancement of heavy daily snowfall in central Japan due to global warming as projected by large ensemble of regional climate simulations. *Clim Change* 139:265–278. <https://doi.org/10.1007/s10584-016-1781-3>

Kawase H, Sasai T, Yamazaki T et al (2018) Characteristics of synoptic conditions for heavy snowfall in western to northeastern Japan analyzed by the 5-km regional climate ensemble experiments. *J*

- Meteorol Soc Japan 96:161–178. <https://doi.org/10.2151/jmsj.2018-022>
- Kawase H, Imada Y, Sasaki H et al (2019) Contribution of historical global warming to local-scale heavy precipitation in western Japan estimated by large ensemble high-resolution simulations. *J Geophys Res Atmos* 124:6093–6103. <https://doi.org/10.1029/2018jd030155>
- Kazama S, Izumi H, Sarukkalige PR et al (2008) Estimating snow distribution over a large area and its application for water resources. *Hydrol Process* 22:2315–2324. <https://doi.org/10.1002/hyp.6826>
- Kohonen T (1982) Self-organized formation of topologically correct feature maps. *Biol Cybern* 43:59–69. <https://doi.org/10.1007/BF00337288>
- Korhonen J, Kuusisto E (2010) Long-term changes in the discharge regime in Finland. *Hydrol Res* 41:253–268. <https://doi.org/10.2166/nh.2010.112>
- Markoff MS, Cullen AC (2008) Impact of climate change on Pacific Northwest hydropower. *Clim Change* 87:451–469. <https://doi.org/10.1007/s10584-007-9306-8>
- Marks D, Kimball J, Tingey D, Link T (1998) The sensitivity of snow-melt processes to climate conditions and forest cover during rain-on-snow: a case study of the 1996 Pacific Northwest flood. *Hydrol Process* 12:1569–1587. [https://doi.org/10.1002/\(SICI\)1099-1085\(199808/09\)12:10<11%3C1569::AID-HYP682%3E3.0.CO;2-L](https://doi.org/10.1002/(SICI)1099-1085(199808/09)12:10<11%3C1569::AID-HYP682%3E3.0.CO;2-L)
- Milly PCD, Wetherald RT, Dunne KA, Delworth TL (2002) Increasing risk of great floods in a changing climate. *Nature* 415:514–517. <https://doi.org/10.1038/415514a>
- Mizuta R, Murata A, Ishii M et al (2017) Over 5,000 years of ensemble future climate simulations by 60-km global and 20-km regional atmospheric models. *Bull Am Meteorol Soc* 98:1383–1398. <https://doi.org/10.1175/BAMS-D-16-0099.1>
- Mote PW, Parson EA, Hamlet AF et al (2003) Preparing for climate change: the water, salmon, and forests of the Pacific Northwest. *Clim Change* 61:45–88. <https://doi.org/10.1023/A:1026302914358>
- Nohara D, Kitoh A, Hosaka M, Oki T (2006) Impact of climate change on river discharge projected by multimodel ensemble. *J Hydrol Meteorol* 7:1076–1089. <https://doi.org/10.1175/JHM531.1>
- Ohba M (2019) The impact of global warming on wind energy resources and ramp events in Japan. *Atmosphere* 10:265. <https://doi.org/10.3390/atmos10050265>
- Ohba M, Kawase H (2020) Rain-on-Snow events in Japan as projected by a large ensemble of regional climate simulations. *Clim Dyn* 55:2785–2800. <https://doi.org/10.1007/s00382-020-05419-8>
- Ohba M, Sugimoto S (2019) Differences in climate change impacts between weather patterns: Possible effects on spatial heterogeneous changes in future extreme rainfall. *Clim Dyn* 52:4177–4191. <https://doi.org/10.1007/s00382-018-4374-1>
- Ohba M, Sugimoto S (2020) Impacts of climate change on heavy wet snowfall in Japan. *Clim Dyn* 54:3151–3164. <https://doi.org/10.1007/s00382-020-05163-z>
- Ohba M, Kadokura S, Yoshida Y et al (2015) Anomalous weather patterns in relation to heavy precipitation events in Japan during the Baiu season. *J Hydrol Meteorol* 16:688–701. <https://doi.org/10.1175/JHM-D-14-0124.1>
- Ohba M, Kadokura S, Nohara D (2016a) Impacts of synoptic circulation patterns on wind power ramp events in East Japan. *Renew Energy* 96:591–602. <https://doi.org/10.1016/j.renene.2016.05.032>
- Ohba M, Kadokura S, Nohara D, Toyoda Y (2016b) Rainfall downscaling of weekly ensemble forecasts using self-organizing maps. *Tellus A* 68:29293. <https://doi.org/10.3402/tellusa.v68.29293>
- Ohba M, Kadokura S, Nohara D (2018) Medium-range probabilistic forecasts of wind power generation and ramps in Japan based on a hybrid ensemble. *Atmosphere* 9:423. <https://doi.org/10.3390/atmos9110423>
- Ohba M, Arai R, Toyoda Y, Sato T (2020) Construction of impact assessment method of global warming for river runoff in Japan by using a runoff analysis model. CRIEPI Research Report n19009
- Polo I, Ullmann A, Roucou P, Fontaine B (2011) Weather regimes in the Euro–Atlantic and Mediterranean sector, and relationship with West African rainfall over the 1989–2008 period from a self-organizing map approach. *J Clim* 24:3423–3432. <https://doi.org/10.1175/2011JCLI3622.1>
- Reusch DB, Alley RB, Hewitson BC (2007) North Atlantic climate variability from a self-organizing map perspective. *J Geophys Res* 112:D02104. <https://doi.org/10.1029/2006JD007460>
- Sasai T, Kawase H, Kanno Y et al (2019) Future projection of extreme heavy snowfall events with a 5-km large ensemble regional climate simulation. *J Geophys Res Atmos* 124:13975–13990. <https://doi.org/10.1029/2019JD030781>
- Singh D, Coauthors (2014) Severe precipitation in northern India in June 2013: causes, historical context, and changes in probability [in “Explaining Extremes of 2013 from a Climate Perspective”]. *Bull Am Meteorol Soc* 95:S58–S61. <https://doi.org/10.1175/1520-0477-95.9.S1.1>
- Sperna Weiland FC, van Beek LPH, Weerts AH, Bierkens MFP (2012) Extracting information from an ensemble of GCMs to reliably assess future global runoff change. *J Hydrol* 412:66–75. <https://doi.org/10.1016/j.jhydrol.2011.03.047>
- Surfleet CG, Tullos D (2013) Variability in effect of climate change on rain-on-snow peak flow events in a temperate climate. *J Hydrol* 479:24–34. <https://doi.org/10.1016/j.jhydrol.2012.11.021>
- Tachibana Y (1995) A statistical study of the snowfall distribution on the Japan Sea side of Hokkaido and its relation to synoptic-scale and meso-scale environments. *J Meteorol Soc* 73:697–715. [https://doi.org/10.2151/jmsj1965.73.3\\_697](https://doi.org/10.2151/jmsj1965.73.3_697)
- Tachikawa Y, Miyawaki K, Tanaka T et al (2017) Future change analysis of extreme floods using large ensemble climate simulation data. *J Jpn Soc Civ Eng B1(73):77–90*
- Tan A, Adam JC, Lettenmaier DP (2011) Change in spring snowmelt timing in Eurasian Arctic rivers. *J Geophys Res* 116:D03101. <https://doi.org/10.1029/2010JD014337>
- Toyoda Y, Sato T, Ishii T, Arai R (2015) The evaluation of small hydroelectric generation unit price in a mountain stream through the use of runoff analysis. *J Jpn Soc Civ Eng G* 71:247–255
- Toyoda Y, Kobayashi T, Shimogaki H (2006) Development of Runoff Model Considering the evapotranspiration Process in forest basin. CRIEPI Research Report n05003
- Troccoli A, Dubus L, Haupt SE (2014) *Weather matters for energy*. Springer, New York
- Vörösmarty CJ, Green P, Salisbury J, Lammers RB (2000) Global water resources: vulnerability from climate change and population growth. *Science* 289:284–288. <https://doi.org/10.1126/science.289.5477.284>
- Yamazaki A, Honda M, Kawase H (2019) Regional snowfall distributions in a Japan-Sea side area of Japan associated with jet variability and blocking. *J Meteorol Soc Japan* 97:205–226. <https://doi.org/10.2151/jmsj.2019-012>

**Publisher's Note** Springer Nature remains neutral with regard to jurisdictional claims in published maps and institutional affiliations.